Journal of Molecular Structure 1149 (2017) 882–892

Contents lists available at ScienceDirect

Journal of Molecular Structure

journal homepage: http://www.elsevier.com/locate/molstruc

Experimental and theoretical analysis of 2-amino 1-methyl benzimidazole molecule based on DFT

E.B. Sas [a, *], M. Cevik [b], M. Kurt [b]

[a] Technical Sciences Vocational Schools, Ahi Evran University, Kırsehir, Turkey
[b] Department of Physics, Ahi Evran University, Kırsehir, Turkey

ARTICLE INFO

Article history:
Received 17 April 2017
Received in revised form
6 July 2017
Accepted 20 July 2017
Available online 8 August 2017

Keywords:
2-Amino 1-methyl benzimidazole
Density functional theory
FT-Raman
FT–IR
Dispersive Raman

ABSTRACT

In this work were shown spectroscopic properties, molecular structure and electronic properties of 2-amino 1 methyl benzimidazole molecule. The theoretical calculations in the title molecule were performed with density functional theory method. Experimental wavenumber of 2-amino 1 methyl benzimidazole molecule were recorded with FT-Raman, dispersive Raman and FT-IR between 4000 and 0, 4000–400 and 4000-370 cm^{-1}, respectively. The scaled theoretical wavenumber are assigned based on total energy distribution. Other experimental spectra were recorded in specific solvents.

1. Introduction

Benzimidazole and its derivatives play important role in industrial and medical fields because of antiviral and parasitic activities. Their biological activities such as antiviral, anticancer, antimalarial, anti-helmintic, antihistaminic, antiulcer, antifungal and anti-oxidant have been studied [1–9]. This compounds are also used broadly in industrial processes as corrosion protection for alloy and metal surfaces [10,11]. Metal complexes including benzimidazole are subject of intensive searches not only because of their opulent coordination chemistry. To examine features of benzimidazole [12–14] and its derivatives [15] study was done many theoretician and experimentalists because of these different applications. Recently, investigated molecular structure, vibrational spectroscopic of 2-arylaminomethyl-1H-benzimidazole with novel Ni (II) and Zn (II) complexes by Abdel-Ghani et al. [13]. Geometric parameters, spectral band, first-order hyperpolarizability and HOMO, LUMO studies of 2-aminobenzimidazole analyzed by Sudha et al. [14], Noolvi et al. reported synthesis, antimicrobial and cytotoxic activity of 1-methyl-1H-benzimidazol-2-amine [16]. Tlahuext et al. investigated structural and synthesis researches of amino amide salts derivatives of 2-(aminomethyl) benzimidazole [17]. Optimized parameter and spectral analysis of 4-chloro-7-nitrobenzofurazan were calculated by Kurt et al. [18].

As a successor to the benzimidazole compounds, theoretical analysis of 2-amino 1 methyl benzimidazole (2A1MB) were obtained at the B3LYP/CC-pVDZ level. The experimental spectra (FT-Raman, FT-IR, dispersive Raman, ^{1}H and ^{13}C NMR) recorded solid phase and DMSO solvent. All results are presented herein.

2. Experimental

The infrared spectrum of 2A1MB was recorded in between of 4000–400 cm^{-1}at room temperature using a Bruker IFS 66/S spectrometer. Thermo Scientific Nicolet 6700 FT-IR/NXR FT-Raman Modül instrument using 1064 nm excitation from an Nd:YAG laser was used and measured in between of 4000-0 cm^{-1}. ^{1}H and ^{13}C NMR chemical shift values were performed in Bruker Superconducting FT.NMR Spectrometer Avance TM. Chemical shifts were measured in ppm connected to tetramethylsilane (TMS) in DMSO. NMR spectra were observed at the base frequency of 300 MHz for ^{13}C and ^{1}H nuclei.

2.1. Calculations

The molecular geometry of 2A1MB was optimized by DFT/B3LYP

* Corresponding author. Tel.: +90 0386 280 4748.
E-mail address: baburemine@gmail.com (E.B. Sas).

http://dx.doi.org/10.1016/j.molstruc.2017.07.055
0022-2860/

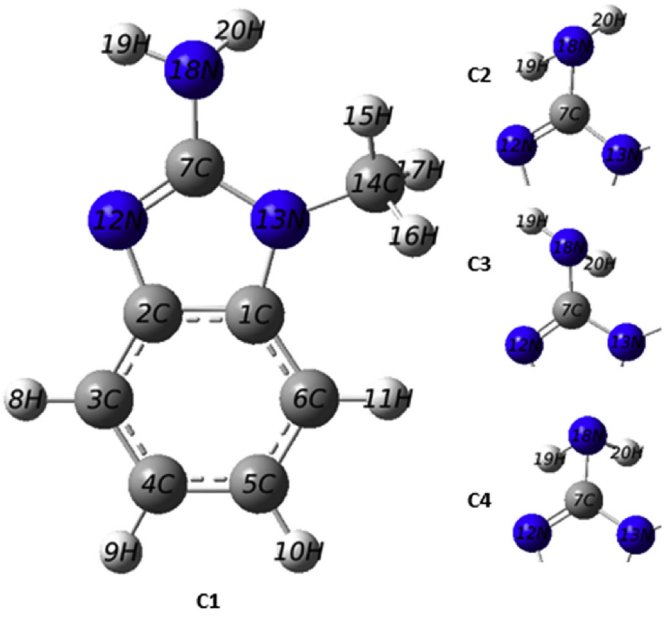

Fig. 1. The theoretical geometric conformers of the 2-amino 1 methyl benzimidazole.

methods by using CC-pVDZ basis set. The vibrational bands were obtained with same basis set. Theoretical vibrational bands were scaled using the scale factor of 0.970 [19]. The vibrational bands were assigned on the basis of TED performed with SQM program [20]. The electronic spectrum of 2A1MB was obtained by TD-DFT method [21]. HOMO-LUMO were calculated at the same level of theory. The ^{1}H and ^{13}C chemical shifts were computed at the B3LYP/CC-pVDZ level of the gas phase by using GIAO approach [22] and the values were referenced to TMS, which was computed at the same level of theory. The calculations were carried out using GAUSSIAN09 [23] software.

3. Results and discussion

3.1. Geometrical structure

All possible conformers of 2A1MB molecule calculated using DFT theory at B3LYP/CC-pVDZ level and optimized energies were given in the Table S1. The optimized energy of other conformers is higher than those of conformer 1 and given in Fig. 1. The dimer structure of conformer 1 is shown in Fig. S1. Geometrical parameters values of conformer 1 are tabulated in Table 1. This parameters, since the crystal structure of the title compound is not available, are compared with analogous optimized compound and x-ray data [24,25]. But we compared geometrical parameters of the title compound and N-Methyl-2-(2'-hydroxyphenyl)benzimidazole X-ray data (R^2). For example, in analogous compounds C–C bond length were obtained in between of 1.39–1.41 Å [25] and in x-ray data were observed in between of 1.37–1.40 Å in phenyl ring [24] and bond length C–C of 2A1MB were calculated in the range of 1.40–1.42 Å. Moreover, bond lengths N13–C14 was calculated at 1.45 Å and in x-ray data of similar molecule were observed as 1.45.The N12–C7–N13 bond angle of the 2A1MB was obtained as 114.22° and as 114.7° in similar molecule [24].

Table 1
Calculated optimized parameter values of the 2-amino 1 methyl benzimidazole [Bond length in (Å), Bond angle in (°)].

	2A1MB	2Br1HB	X-Ray	R^2		2A1MB	2Br1HB	X-Ray	R^2
Bond Length									
C1–C2	1.419	1.414	1.4	−1.3	C6–H11	1.092	1.084	0.93	−14.8
C1–C6	1.395	1.393	1.386	−0.6	C7–N12	1.314	1.294	1.338	1.8
C1–N13	1.393	1.388	1.395	0.1	C7–N13	1.384	1.374	1.352	−2.3
C2–C3	1.400	1.397	1.387	−0.9	C7–N18	1.391	–	–	–
C2–N12	1.391	1.394	1.377	−1.0	N13–C14	1.447	–	–	–
C3–C4	1.397	1.39	1.374	−1.6	C14–H15	1.099	–	–	–
C3–H8	1.092	1.083	0.93	−14.8	C14–H16	1.101	–	–	–
C4–C5	1.408	1.407	1.392	−1.1	C14–H17	1.104	–	–	–
C4–H9	1.092	1.084	0.93	−14.8	N18–H19	1.019	–	–	–
C5–C6	1.399	1.391	1.368	−2.2	N18–H20	1.020	–	–	–
C5–H10	1.092	1.084	0.93	−14.8					
Bond Angle									
C2–C1–C6	122.7	122.6	120.6	−1.7	C5–C6–H11	121.1	121.3	121.1	0.0
C2–C1–N13	105.0	104.5	108.1	3.0	N12–C7–N13	114.3	114.7	112.7	−1.4
C6–C1–N13	132.2	132.9	131.2	−0.8	C12–C7–N18	124.9	–	–	–
C1–C2–C3	119.5	119.9	121.3	1.5	N13–C7–N18	120.7	–	–	–
C1–C2–N12	110.5	110.4	107.2	−3.0	C2–N12–C7	104.4	104.4	107	2.5
C3–C2–N12	130.1	129.7	131.5	1.1	C1–N13–C7	105.8	106.1	105.1	−0.7
C2–C3–C4	118.3	117.8	117.3	−0.8	C1–N13–C14	127.0	–	–	–
C2–C3–H8	120.1	120.4	121.4	1.1	C7–N13–C14	127.1	–	–	–
C4–C3–H8	121.6	121.8	121.4	−0.2	N13–C14–H15	109.0	–	–	–
C3–C4–C5	121.4	121.5	121.4	0.0	N13–C14–H16	109.8	–	–	–
C3–C4–H9	119.4	119.5	119.3	−0.1	N13–C14–H17	112.2	–	–	–
C5–C4–H9	119.1	119.1	119.3	0.2	H15–C14–H16	108.2	–	–	–
C4–C5–C6	121.2	121.6	121.7	0.4	H15–C14–H17	109.2	–	–	–
C4–C5–H10	119.5	119.3	119.2	−0.3	H16–C14–H17	108.4	–	–	–
C6–C5–H10	119.3	119.1	119.2	−0.1	C7–N18–H19	109.3	–	–	–
C1–C6–C5	116.8	116.6	117.8	0.9	C7–N18–H20	113.8	–	–	–
C1–C6–H11	122.1	122.1	121.1	−0.8	H19–N18–H20	109.6	–	–	–

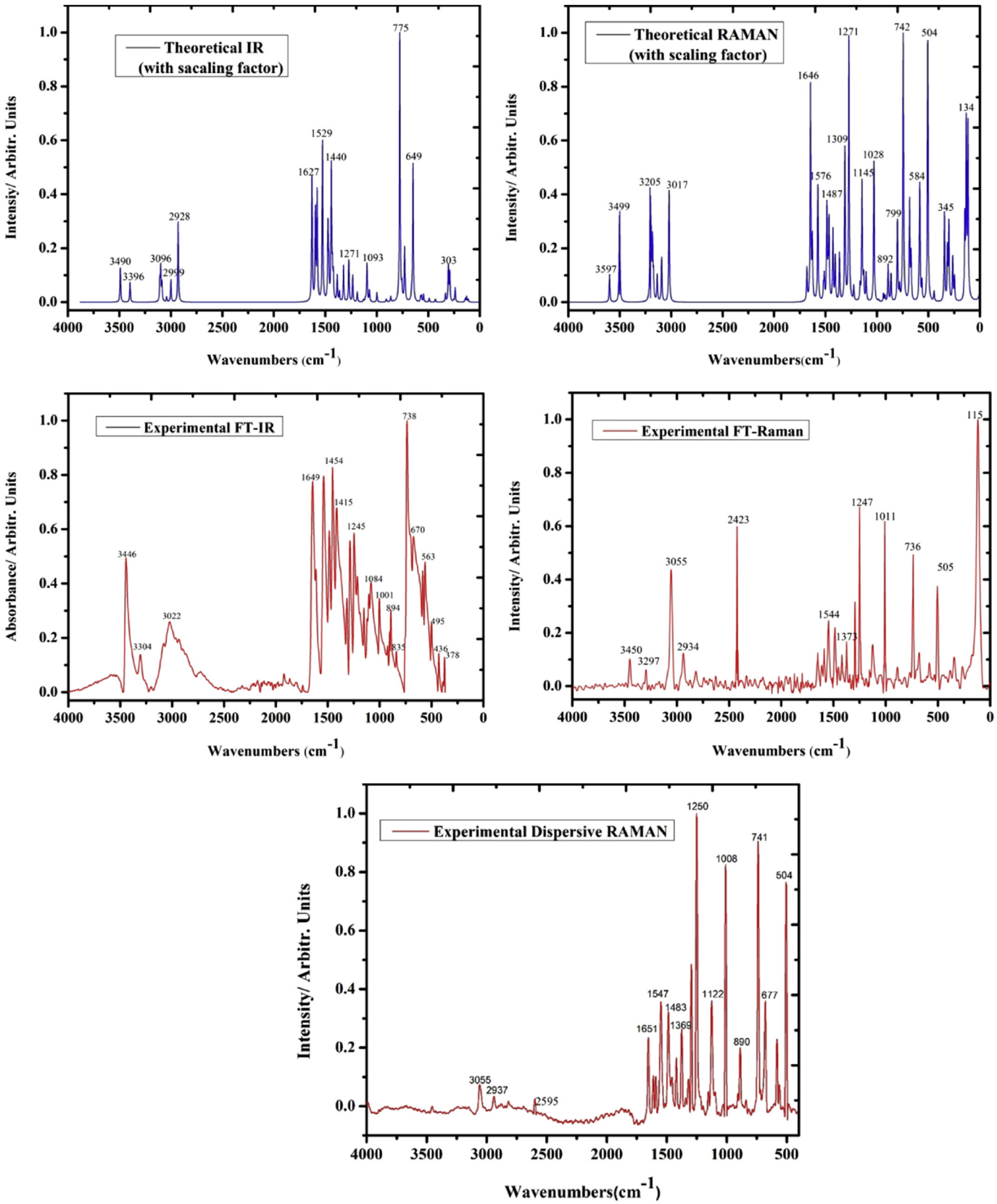

Fig. 2. The experimental and calculated (with the scale factor) FT-IR and FT-Raman spectra of the2-amino 1 methyl benzimidazole.

Table 2
Comparison of the calculated and experimental vibrational spectra and proposal assignments of 2-amino 1 methyl benzimidazole molecule.

No	Experimental wavenumber			Theoretical wavenumber				TED (≥10%)
	FT-IR	FT-Raman	Dispersive Raman 780nm	Scaled	I_{IR}	S_{Ra}	I_{Ra}	Assignments[a]
1		115		113	2.31	1.37	1.00	τCCCN(29)+ τCCNN(28)+τCCHN(34)
2				129	4.25	1.61	0.92	τCCCN(19)+ τCCHN(56)
3				143	2.64	0.82	0.39	τCCCN(35)+ τCCNN(28)+ τCCHN(23)
4				240	10.75	0.45	0.09	δCCN(51)
5				257	1.26	0.88	0.16	τCCCC(15)+ τCCCN(20)+ τCCNN(13)
6				292	21.85	1.82	0.26	δCCN(27)+ τCHNN(37)
7				305	26.82	1.28	0.17	δCCN(18)+δCNN(21)+τCHNN(37)
8	378			334	6.23	2.47	0.29	τCCCC(17)+ τCCCN(25)+ τCCNN(28)
9	436			431	2.35	0.37	0.03	τCCCC(35)+ ΓCCCH(19)+ τCCCN(29)
10	495	505	504	491	3.06	11.76	0.77	υCC(13)+υCN(22)+δCCC(23)
11				547	5.87	0.95	0.05	δCCN(51)+δCNN(18)
12	563			567	4.25	6.37	0.34	δCCC(28)+δCCN(27)+δCNN(13)
13				575	3.60	0.68	0.04	τCCCC(42)+ τCCCH(14)+ τCCCN(15)
14				649	103.33	2.95	0.13	τCCNN(21)+ΓCHNN(30)
15	670		677	663	5.24	6.81	0.29	υCN(14)+δCCC(20)+δCCN(19)
16				722	3.95	20.36	0.76	υCC(20)+υCN(37)+δCCC(15)
17	738	736	741	730	39.48	1.89	0.07	γ ΓCCCH(73)+ τCCHN(16)
18				757	9.25	1.13	0.04	τCCCC(28)+ τCCCH(28)+ τCCNN(11)
19				777	201.32	6.97	0.23	δCNH(22)+ ΓCHNN(51)
20	835			837	0.43	2.67	0.08	τCCCC(10)+ γ [ΓCCCH(31)+ ΓCCHH(17)] + τCCHN(28)
21				865	4.13	3.84	0.11	υCC(19)+υCN(19)+δCCC(19)+δCCN(10)
22	894		890	895	0.33	0.65	0.02	υCN(41)+δCHN(12)
23				909	2.15	0.89	0.02	γ[ΓCCCH(30)+ ΓCCHH(44)]+ ΓCCHN(15)
24				954	0.09	0.22	0.01	γ[ΓCCCH(20)+ ΓCCHH(63)]
25	1001	1011	1008	998	7.42	18.35	0.43	υCC(60)+δCCH(27)
26				1071	8.59	4.17	0.09	υCC(11)+υCN(17)+δCCC(10)+δCCH(16) +δCHN(10)
27	1084			1095	28.50	3.42	0.07	υCC(11)+ δCCH(16)+δCHN(40)
28				1101	3.76	1.11	0.02	δCHN(66)+ ΓCCHN(18)
29				1111	2.12	18.72	0.37	υCC(10)+υCN(10)+δCCH(20)+δCHN(29)
30			1122	1129	1.63	2.34	0.05	υCC(16)+ δCCH(74)
31				1189	7.49	2.62	0.05	υCN(20)+δCCH(10)+δCHN(24)
32	1245	1247	1250	1235	20.10	50.19	0.84	υCC(18)+υCN(41)+δCCH(17)
33				1272	31.61	30.77	0.49	υCN(21)+ δCCH(53)
34				1323	27.14	10.34	0.15	υCC(19)+υCN(46)
35		1373	1369	1363	7.56	10.28	0.15	υCC(49)+δCCH(14)
36				1385	19.44	16.99	0.23	δCHH(39)+δCHN(37)
37	1415			1422	18.62	19.73	0.26	δCHH(56)+δCHN(11)+ ΓCCHN(27)
38				1431	21.68	6.73	0.09	δCHH(39)+ ΓCCHN(19)
39	1454			1442	102.15	24.68	0.32	υCC(27)+υCN(10)+δCCH(30)
40				1466	23.86	6.51	0.08	υCC(30)+υCN(12)+δCCH(29)
41			1483	1474	55.81	3.75	0.05	υCN(34)+δCHH(16)+δCHN(10)
42		1544	1547	1527	119.99	33.67	0.39	υCN(38)+δCHN(17)+ δHNN(22)
43				1579	81.17	18.44	0.20	υCN(43)+δCHN(10)+δHNN(17)
44				1596	67.83	69.83	0.75	υCC(44)+υCN(14)+ δHNN(12)
45	1649		1651	1630	93.85	11.05	0.11	υCC(43)+υCN(22)
46		2423	2595	2929	60.29	193.71	0.54	υCH(100)sm
47		2934	2937	3000	16.97	84.13	0.22	υCH(100) asm
48	3022	3055	3055	3041	3.78	53.31	0.13	υCH(98) asm
49				3076	0.02	50.13	0.12	υCH(100) asm
50				3086	13.61	122.31	0.29	υCH(97) asm
51				3098	25.48	97.72	0.23	υCH(98) asm
52				3107	14.98	292.57	0.68	υCH(99) sm
53	3304	3297		3396	15.09	310.75	0.55	υNH(100) sm
54	3446	3450		3491	25.95	96.68	0.16	υNH(100) asm

[a] υ : stretching. δ : bending.δ :in plane bending.γ : out of plane bending. Γ : torsion.

3.2. Vibrational spectral analysis

The title of molecule has 20 atoms and 54 vibrational band. The theoretical IR and Raman spectrum of 2A1MB were performed at DFT method of theory using CC-pVDZ basis set as given in Fig. 2 with experimental Raman and IR spectra. All band assignments were presented in Table 2. Vibrational modes were performed with detailed based on the total energy distribution (TED). In this study, the scaling factor is 0.970 for B3LYP/CC-pVDZ basis set. Correlation graphics between the experimental and theoretical wavenumber were plotted in Fig. S2.

3.2.1. CH_3 vibrations

The C–H stretching of CH_3 groups are expected to be at lower frequencies than those of aromatic ring (3100–3000 cm^{-1}). The asymmetric stretch is usually observed at higher wavenumber than the symmetric stretch. The asymmetric C–H stretching mode of CH_3 is expected around 2980 cm^{-1} and symmetric C–H stretching mode of CH_3 should beat 2870 cm^{-1} from previous works in the literature [26–28]. Asymmetric stretching vibrations of CH_3 of 2A1MB were calculated at 3000 cm^{-1} and it was observed at 2934 cm^{-1} in FT–Raman and 2937 cm^{-1} in dispersive Raman spectrum. The CH_3 symmetric stretching vibration was calculated at 2929 cm^{-1} but it was observed at 2423 cm^{-1} in FT–IR and 2595 cm^{-1} in dispersive Raman spectrum. These vibrations show 100% of PED contribution suggesting that it is a pure stretching mode. Scissoring vibrations of CH_3 were calculated at 1474, 1431, 1421 and 1384 cm^{-1} with B3LYP/CC-pVDZ method.

3.2.2. C–H vibrations

C–H stretching vibrations generally occurs in between of 3000–3100 cm^{-1} in hetero aromatic rings [29–32]. The C–H stretching vibrations were computed in the region between 3041 and 3107 cm^{-1} were observed at 3022, 3055 and 3055 cm^{-1} in FT–IR, FT-Raman and dispersive Raman. The C–H in–plane bending and out of plane bending vibrations occurs in the ranges 1000–1300 cm^{-1} and 800-950 cm^{-1} for aromatic rings, respectively [33,34]. The C–H in–plane bending and out of plane bending vibrations for 2A1MB molecule were calculated in the range of 999–1271 cm^{-1} and at 837, 909 and 954 cm^{-1}, respectively. These vibrations observed at 835, 1001 cm^{-1} in FT-IR and at 1011 cm^{-1} in FT-Raman and 1008, 1122 cm^{-1} in dispersive Raman spectrum. These vibrations in similar molecules also calculated and observed in the ranges same band [23,35–38].

3.2.3. NH_2 vibrations

N–H stretching vibrations generally occurs in between of 3300–3500 cm^{-1} in aromatic amines [39]. The N–H asymmetric and symmetric vibrational stretching modes were computed at 3491 and 3396 cm^{-1} for monomer. These bands were computed at 3487 and 3487 cm^{-1} for dimer structure. Therefore the modes were showed downshift due to the inter-molecular effect. The observed experimental FT-Raman and FT-IR spectrum as two bands at 3297, 3450 and 3304, 3446 cm^{-1}, respectively. These vibrations show 100% of PED contribution suggesting that it is a pure stretching mode. Bellamy et al. have reported that the NH_2 scissoring vibration mode lies in between of 1529–1650 cm^{-1} [40,41]. The NH_2 scissoring mode of 2A1MB were calculated in between of 1527–1596 cm^{-1} and observed at 1544 and 1547 cm^{-1} in FT-Raman and dispersive Raman spectrum.

3.2.4. Ring vibrations

The bands generally in between of 1480 and 1650 cm^{-1} are assigned to C–C stretching modes [42]. This band for 2A1MB was observed at 1649, 1454, 1245, 1084, 1001 cm^{-1}in FT-IR and at 1343, 1247, 1011 cm^{-1} in FT-Raman and at 1651, 1369, 1250, 1122, 1008 cm^{-1} in dispersive Raman. C–C stretching modes were obtained in the ranges 1630–1596, 1466–1442, 1363–1323, 1234, 1189–1112, 1097-999 $cm^{-1}$by CC-pVDZ basis set. The main C–C stretching vibration were calculated at 999 cm^{-1} with the TED contribution 60%.

3.2.5. C–N vibrations

C=N stretching band generally occurs in the range of 1672-1566 cm^{-1} [24]. C=N stretching mode reported by Arjunan et al., at 1531 $cm^{-1}$for 2-amino-4-methylbenzothiaole [43]. This band was calculated at 1527, 1596 and 1630 cm^{-1} observed at 1649 and 1544 and 1547, 1651 cm^{-1} in FT-IR, FT-Raman and dispersive Raman

Table 3
Experimental and calculated chemical shifts (ppm).

Atom	B3LYP/CC-pVDZ				Experimental
	DMSO	Ethanol	Gas	Water	DMSO
C7	142.04	141.94	138.97	142.08	155.84
C2	131.40	131.43	132.07	131.39	142.92
C1	125.44	125.41	124.65	125.45	135.41
C4	109.49	109.52	110.67	109.47	120.74
C5	108.72	108.72	109.19	108.72	118.46
C3	105.32	105.41	107.69	105.28	115.09
C6	97.14	97.08	95.71	97.17	107.76
C14	18.64	18.62	18.28	18.64	28.81
H8	7.74	7.75	7.82	7.74	7.12
H11	7.61	7.60	7.33	7.62	6.94
H9	7.58	7.58	7.54	7.58	6.98
H10	7.55	7.55	7.45	7.55	7.18
H15	4.12	4.12	4.01	4.13	3.51
H16	4.08	4.08	4.00	4.08	3.51
H19	4.05	4.04	3.85	4.05	6.57
H17	3.78	3.77	3.57	3.78	3.51
H20	3.59	3.56	2.88	3.60	6.57

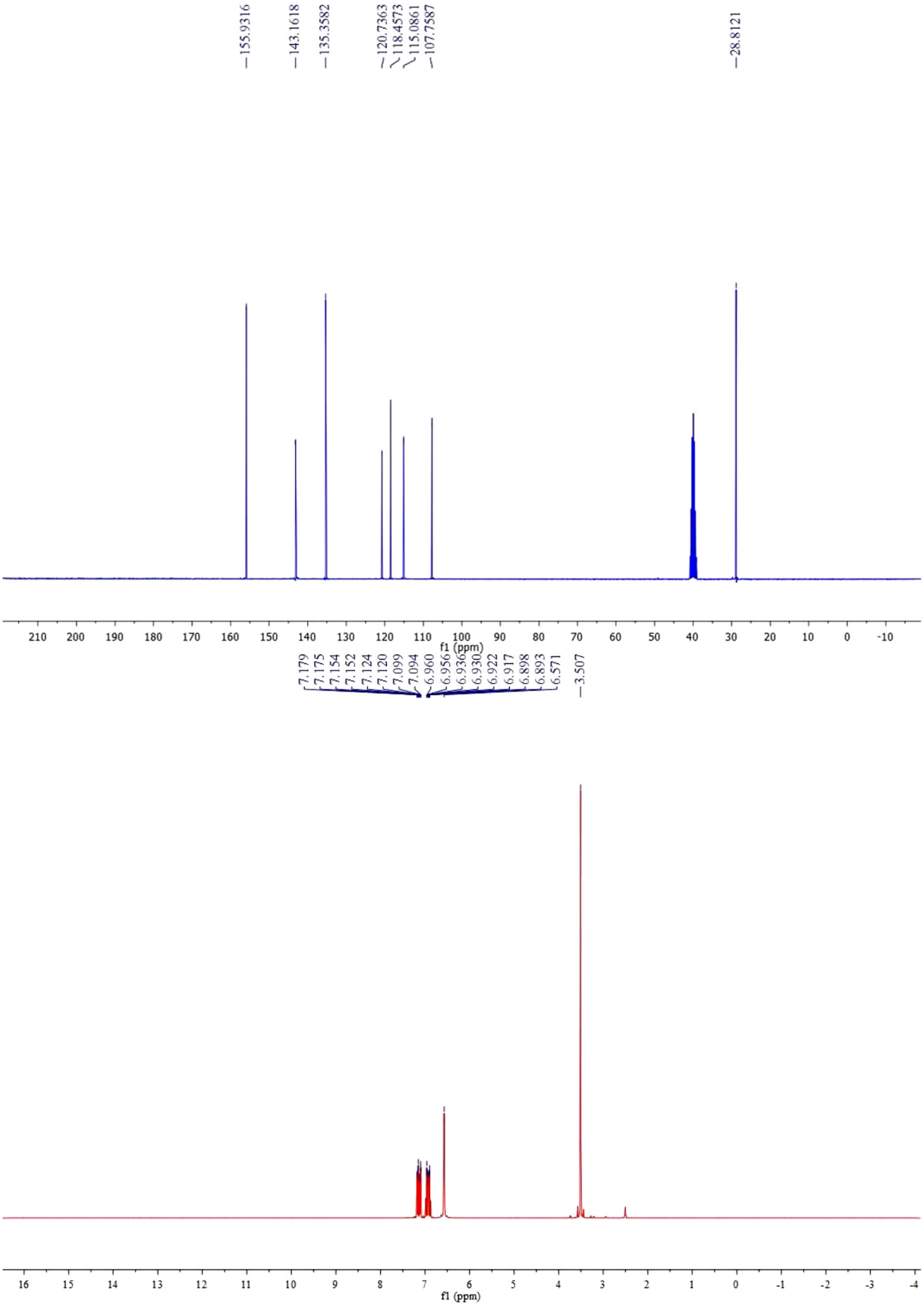

Fig. 3. ^{1}H and ^{13}C NMR spectra of 2-amino 1 methyl benzimidazole in dimethyl sulfoxide solution.

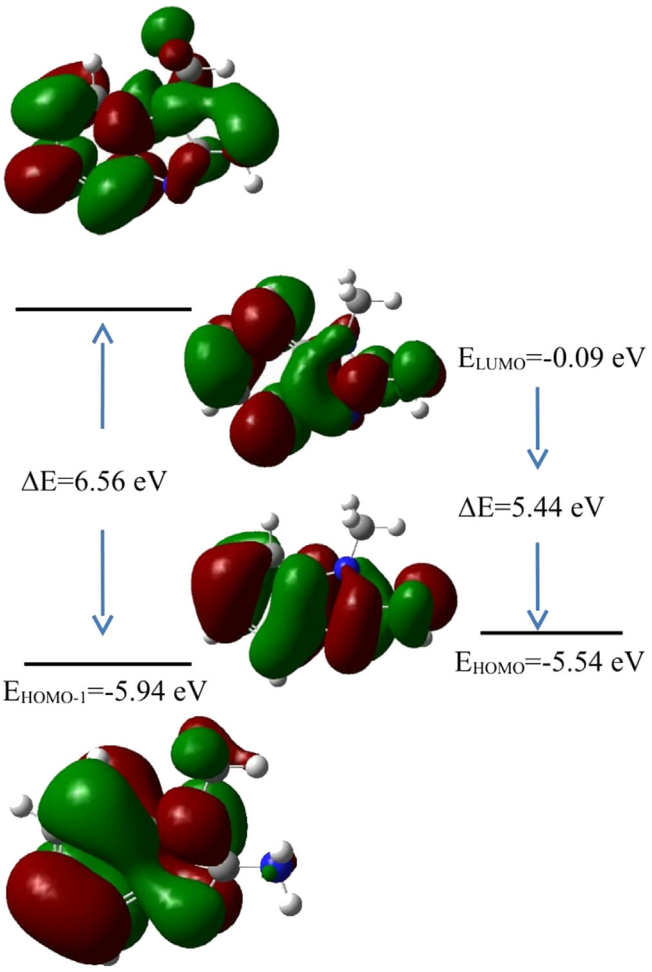

Fig. 4. The frontier molecular orbitals of the 2-amino 1 methyl benzimidazole for gas phase.

spectrum, respectively.

In according to TED, C–N stretching mode looks coupled with C–C vibration. The C–N stretching bands by the Sundaraganesan et al. reported at 1318 cm^{-1} for benzothiazole [44]. This vibration mode in 1-Methyl-2-(2′-hydroxyphenyl)benzimidazole molecule were observed at 1294, 1380 cm^{-1} in FT-IR calculated at 1259, 1349 cm^{-1} by B3LYP/6.31G(d,p) level [24]. For 2A1MB molecule the calculated bands at 1071, 1112, 1189, 1271, 1323, 1442 and 1466 cm^{-1} are assigned to C–N stretching, in which 1323 cm^{-1} have TED of 46%. The experimentally value of C–N stretching vibration observed at 1454 cm^{-1} in FT-IR.

3.3. Nuclear magnetic resonance analysis

The signals of aromatic carbons reported in the range 100–200 ppm [45,46]. The experimental chemical shift of aromatic carbons of the title molecule recorded in between of 114.53–143.80 ppm and those theoretical shift values predicted in the range of 97.14–131.40 ppm in DMSO. The C6 atom is slightly lesser due to effect of nitrogen in the hetero ring, thus its NMR signal is found in the downfield at 97.14 ppm. ^{13}C and ^{1}H NMR chemical shift values calculated by CC-pVDZ basis set and GIAO method were presented in Table 3. ^{1}H chemical shifts were obtained in the range of 7.55–7.74 ppm, whereas the experimental shifts are observed in the range of 8.34–7.34 ppm. The obtained chemical shifts are in good agreement with experimental shifts. The measured ^{13}C and the ^{1}H NMR spectra are shown in Fig. 3. Correlation graphics between the experimental and theoretical chemical shifts were plotted in Fig. S3.

3.4. Frontier molecular orbitals

The HOMO-LUMO energy orbital values play an important role in the electrical and optical properties [47]. The energy values of the HOMO and LUMO orbitals for 2A1MB are presented in Fig. 4 in gas phase. HOMO and LUMO energy values calculated by using TD–DFT/B3LYP/CC-pVDZ are presented in Table 4. The HOMO-LUMO orbitals are localized in the whole of molecule except CH_3 atoms. The energy difference between HOMO and LUMO is a critical parameter in determining molecular electrical transport properties [48]. The energy gap of HOMO and LUMO is found to be 5.44 eV by using TD–DFT/B3LYP/CC-pVDZ. Bold characters in the table indicates energy gap values. The values chemical harness, chemical potential, electronegativity and electrophilicity index for 2A1MB were also calculated and are given Table 4.

3.5. Molecular electrostatic potential surface

MEP provides the investigation of the molecular structure with

Table 4
The calculated energies values of 2-amino 1 methyl benzimidazole molecules using by the B3LYP method using CC-pVDZ basis set.

Parametres	Gas	DMSO	Ethanol	Water
E_{total} (Hartree)	−474.569944	−474.581311	−474.402878	−474.40341
E_{HOMO} (eV)	−5.54	−5.76	−5.75	−5.77
E_{LUMO} (eV)	−0.09	−0.33	−0.32	−0.33
E_{HOMO-1} (eV)	−5.94	−6.16	−6.15	−6.17
E_{LUMO+1} (eV)	0.62	0.39	0.4	0.38
$E_{HOMO-1–LUMO+1\ gap}$ (eV)	**−6.56**	**−6.56**	**−6.55**	**−6.55**
$E_{HOMO–LUMO\ gap}$ (eV)	**−5.44**	**−5.44**	**−5.44**	**−5.44**
Chemical hardness (h)	−2.72	−2.72	−2.72	−2.72
Electronegativity (χ)	2.82	3.04	3.04	3.05
Chemical potential (μ)	−2.82	−3.04	−3.04	−0.305
Electrophilicity index (ω)	−1.46	−1.7	−1.69	−1.71

Bold text indicates energy gap and it is critical parameter.

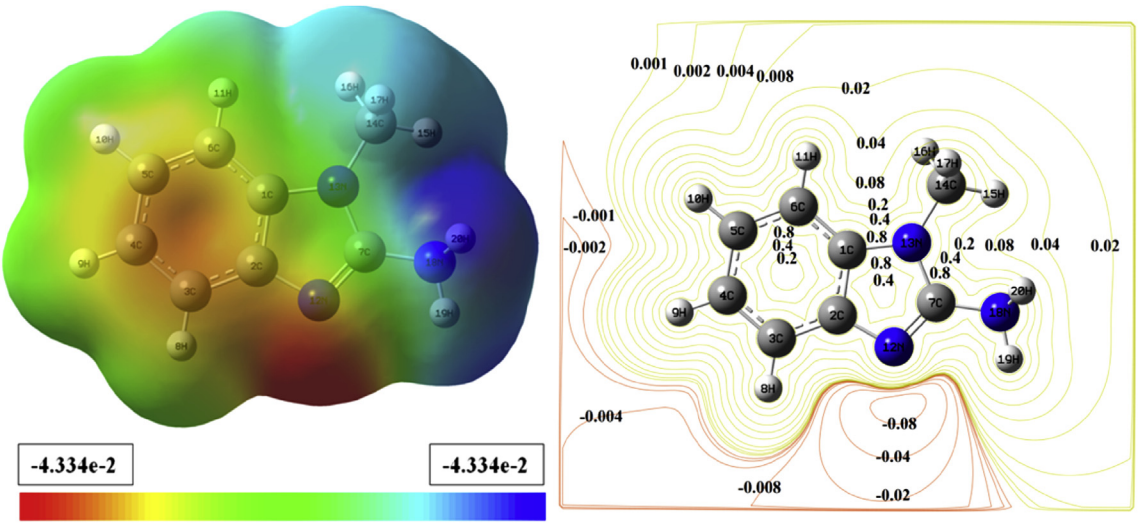

Fig. 5. Molecular electrostatic potential (MEPs) 3D map and 2D contour map for 2-amino 1 methyl benzimidazole molecule.

Table 5
Comparison of Mulliken charges of 2-amino 1 methyl benzimidazole, 2-bromo-1h-benzimidazole and Benzimidazole.

Atoms	2A1MB	2Br1HB	Benzimidazole
C1	0.136	0.505	0.616
C2	0.033	0.912	0.515
C3	0.003	−0.807	−0.680
C4	0.036	−0.186	−0.189
C5	0.029	−0.290	−0.274
C6	0.001	−0.956	−0.687
C7	0.185	0.241	0.230
H8	−0.040	0.131	0.129
H9	−0.038	0.128	0.125
H10	−0.039	0.128	0.125
H11	−0.044	0.116	0.113
N12	−0.251	−0.069	−0.186
N13	−0.264	−0.153	−0.261
C14	0.068	0.329	0.301
H15	0.039	–	–
H16	0.047	–	–
H17	0.038	–	–
N18	−0.147	–	–
H19	0.105	–	–
H20	0.101	–	–

its physiochemical property relationships [49–52]. 2D contour map provides predicting the interaction of different geometries [53–59]. The negative (red) regions and positive (blue) regions shows electrophilic reactivity and nucleophilic reactivity, respectively. The color code maps for 2A1MB were predicted in between of −0.05334 (deepest red) and 0.05334 a.u. (deepest blue), as shown in Fig. 5. As seen, indicates that the region around the nitrogen atom (N12) linked with carbon through the double bond is the most negative potential region (red) and the hydrogen atom linked with nitrogen (N18) is the most bang of positive region (blue).

3.6. Mulliken atomic charges

Mulliken atomic charges of the title molecule were computed by B3LYP/CC-pVDZ method and with 2-bromo 1-h benzimidazole [23] and benzimidazole were tabulated in Table 5. The comparison of the Mulliken charge distribution of molecules were shown in Fig. 6. All in compounds nitrogen atoms have negative charge and N12 nitrogen atom has the high negative charge. This may be due to N–H.N intermolecular interaction. The carbon atoms in 2A1MB have positive charges while C6 has negative charge, however, the other molecules only C1/C2/C7 have positive charge. It may be the reason of the substitution of electronegative methyl groups on C14 atom. H19 atom has the high positive charge. This may be due to amino group intermolecular interaction.

3.7. Thermodynamic properties

Thermodynamic parameters obtained by B3LYP/CC-pVDZ method at 298.15 K for 2A1MB were tabulated in the Table S2. Parameters as heat capacity at constant pressure, entropy and enthalpy changes were calculated in the temperature range of 100–700 K varied every 50 K are presented in Table S3.Thermodynamic parameters enhancement with the rise of temperature because to molecular vibrational intensity enhancement by temperature. The correlation graphics of temperature dependence of thermodynamic functions for the title compound molecule are given in Fig. 7. The correlation equations between heat capacity, entropy, enthalpy changes and temperatures are fitted by quadratic formulas. From the Fig. 7, it can be observed that these thermodynamic functions are increasing with temperature.

4. Conclusion

Studies have been made for 2A1MB such as geometric optimization, vibrational wavenumbers, NMR, MEP, frontier molecule orbital and thermodynamic properties. This study has been presented using DFT/B3LYP/CC-pVDZ level. The obtained bond lengths and bond angles compared with similar structures and X-ray. The calculated as theoretically IR and Raman spectra compared FT-IR and FT-Raman spectra recorded as experimentally and this values

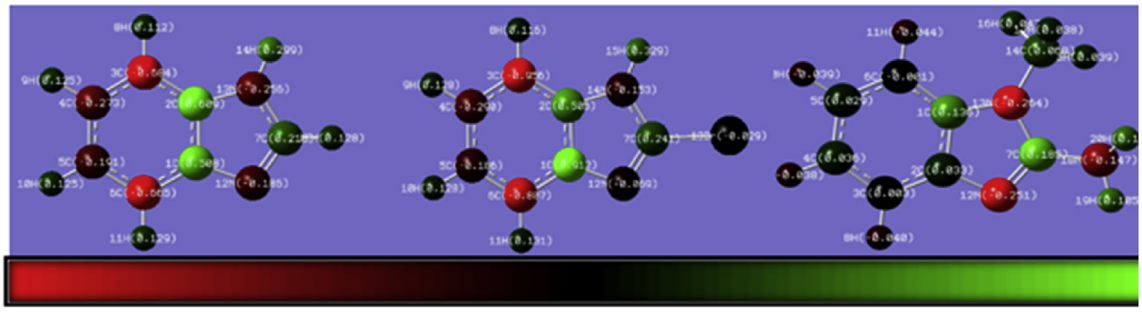

Benzimidazole
Type: Mulliken
Color Range: -0.956 to 0.956

2Br1HB
Type: Mulliken
Color Range: -0.684 to 0.684

2A1MB
Type: Mulliken
Color Range: -0.264 to 0.264

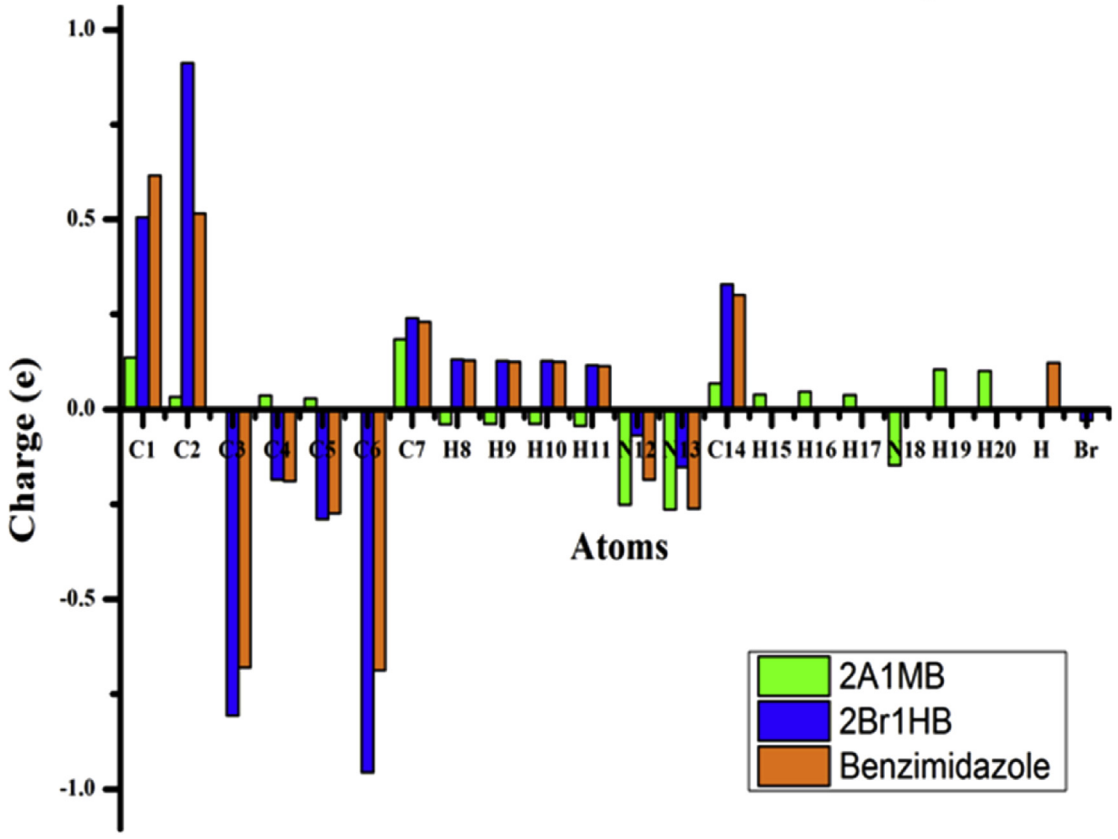

Fig. 6. The Mulliken charge distribution for Benzimidazol, 2-bromo 1h-benzimidazole and 2-amino 1 methyl benzimidazole.

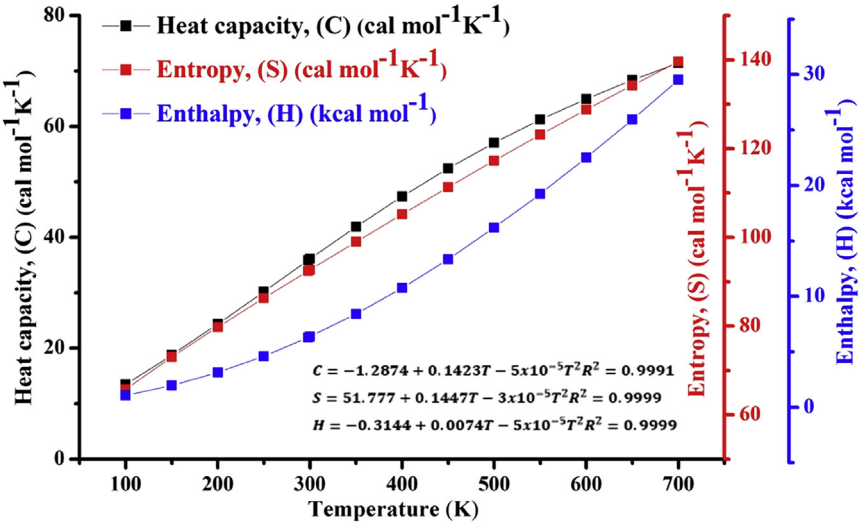

Fig. 7. The correlation graphic of heat capacity, entropy, enthalpy and temperature for 2-amino 1 methyl benzimidazole molecule.

displayed also obtained correlation graphics. Besides, correlation graphics were drawn also for NMR and thermodynamic properties. As it is seen from this graph, experimental and theoretical values are in agreement.

Acknowledgements

This work was supported by Ahi Evran University Scientific Project Unit (BAP) with, Project No: PYO–FEN.4003–12.009.

Appendix A. Supplementary data

Supplementary data related to this article can be found at http://dx.doi.org/10.1016/j.molstruc.2017.07.055.

References

[1] Y. Bansal, O. Silakari, The therapeutic journey of benzimidazoles: a review, Bioorg. Med. Chem. 20 (2012) 6208.
[2] D. Dai, J.R. Burgeson, D.N. Gharaibeh, A.L. Moore, R.A. Larson, N.R. Cerruti, S.M. Amberg, T.C. Bolken, D.E. Hruby, Discovery and optimization of potent broad-spectrum arenavirus inhibitors derived from benzimidazole, Bioorg. Med. Chem. Lett. 23 (2013) 744.
[3] J. Bauer, S. Kinast, A. Burger-Kentischer, D. Finkelmeier, G. Kleymann, W.A. Rayyan, K. Schr∈oppel, A. Singh, G. Jung, K.H. Wiesmüller, S. Rupp, H. Eickhoff, A new class of antimycotic (S)-2-aminoalkyl benzimidazoles exhibits potent antifungal activity against clinically relevant and against fluconazole resistant strains of Candida spp, J. Med. Chem. 54 (2011) 6993.
[4] Y. Yan, Z. Liu, J. Zhang, R. Xu, X. Hu, G. Liu, A reverse method for diversity introduction of benzimidazole to synthesize H(+)/K(+)-ATP enzyme inhibitors, Bioorg. Med. Chem. Lett. 21 (2011) 4189.
[5] J.L. Wang, J. Zhang, Z.M. Zhou, Z.H. Li, W.Z. Xue, D. Xu, L.P. Hao, X.F. Han, F. Fei, T. Liu, A.H. Liang, Design, synthesis and biological evaluation of 6-substituted aminocarbonyl benzimidazole derivatives as nonpeptidic angiotensin II AT1 receptor antagonists, Eur. J. Med. Chem. 49 (2012) 183.
[6] S. Demirayak, I. Kayagil, L. Yurttas, Microwave supported synthesis of some novel 1,3-diarylpyrazino[1,2-a]benzimidazole derivatives and investigation of their anticancer activities, Eur. J. Med. Chem. 46 (2011) 411.
[7] A. Husain, M. Rashid, M. Shaharyar, A.A. Siddiqui, R. Mishra, Benzimidazole clubbed with triazolo-thiadiazoles and triazolo-thiadiazines: new anticancer agents, Eur. J. Med. Chem. 62 (2013) 785.
[8] H.B. El-Nassan, Synthesis, antitumor activity and SAR study of novel [1,2,4]triazino[4,5-a]benzimidazole derivatives, Eur. J. Med. Chem. 53 (2012) 22.
[9] M. Rashid, A. Husain, R. Mishra, Synthesis of benzimidazoles bearing oxadiazole nucleus as anticancer agents, Eur. J. Med. Chem. 54 (2012) 855.
[10] R.W. Walker, The Use of Benzotriazole as a Corrosioninhibitor for Copper-Anticorrosion17, 1970, p. 9.
[11] S. Thiboult, Corros. Sci. 17 (1977) 359.
[12] FabricioGava Fabio da Silva Miranda, Menezes, Juliano Vicente, Adailton J. Bortoluzzi, Cesar Zucco, Ademir Neves, Norberto Sanches Goncalves, bis-(1H-Benzimidazol-2-yl)-methanone: new preparation method, crystal structure, vibrational spectroscopy and DFT calculations, J. Mol. Struct. 938 (2009) 1.
[13] Nour T. Abdel-Ghani, Maha F. Abo El-Ghar, Ahmed M. Mansour, Novel Ni(II) and Zn(II) complexes coordinated by 2-arylaminomethyl-1H-benzimidazole: molecular structures, spectral, DFT studies and evaluation of biological activity, Spectrochim. Acta A 104 (2013) 134.
[14] S. Sudha, M. Karabacak, M. Kurt, M. Cinar, N. Sundaraganesan, Molecular structure, vibrational spectroscopic, first-order hyperpolarizability and HOMO, LUMO studies of 2-aminobenzimidazole, Spectrochim. Acta A 84 (2011) 184.
[15] L. Sinha, O. Prasad, M. Karabacak, H.N. Mishra, V. Narayan, A.M. Asiri, Quantum-chemical (DFT, MP2) and spectroscopic studies (FT-IR and UV) of monomeric and dimeric structures of 2(3H)-Benzothiazolone, Spectrochim. ActaA 120 (2014) 126.
[16] M. Noolvi, S. Agrawal, H. Patel, A. Badiger, M. Gaba, A. Zambre, Synthesis, antimicrobial and cytotoxic activity of novel azetidine-2-one derivatives of 1H-benzimidazole, Arabian J. Chem. 7 (2014) 219–226.
[17] C. Avila-Montiel, A.R. Tapia-Benavides, M. Falcon-Leon, A. Ariza-Castolo, H. Tlahuext, M. Tlahuextl, Synthesis and structural studies of amino amide salts derived from 2-(aminomethyl)benzimidazole and α-amino acids, J. Mol. Struct. 1100 (2015) 338–347.
[18] M. Kurt, Babu P. Chinna, N. Sundaraganesan, Cinar, M. Karabacak, Molecularstructure, vibrational, UV and NBO analysis of 4-chloro-7-nitrobenzofurazan by DFT calculations, Spectrochim. Acta A 79 (2011) 1162–1170.
[19] http://cccbdb.nist.gov/vsfx.asp.
[20] J. Baker, A.A. Jarzecki, P. Pulay, Direct scaling of primitive valence force constants: an alternative approach to scaled quantum mechanical force fields, J. Phys. Chem. A 102 (1998) 1412–1424.
[21] M.E. Casida, J.M. Seminario (Eds.), RecentDevelopments and Applications of Modern DensityFunctionalTheory, Theoretical and ComputationalChemistry, vol. 4, Elsevier, Amsterdam, 1996, p. 391.
[22] R. Ditchfield, Chem. Phys. 76 (1972) 5688–5691.
[23] M.J. Frisch, et al., Gaussian 09, Revision A.1, Gaussian, Inc, Wallingford, CT, 2009.
[24] E.B. Sas, M. Kurt, M. Karabacak, A. Poiyamozhi, N. Sundaraganesan, FT-IR, FT-Raman, dispersive Raman, NMR spectroscopic studies and NBO analysis of 2-Bromo-1H-Benzimidazol by density functional method, J. Mol. Struct. 1081 (2015) 506–518.
[25] H. Saral, Ö. Özdamar, İ. Uçar, Y. Bekdemir, M. Aygün, Synthesis, spectroscopic characterization and DFT calculations of N-Methyl-2-(2′-hydroxyphenyl) benzimidazole derivatives, J. Mol. Struct. 1103 (2016) 9–19.
[26] M. Chen, U.V. Waghmare, C.M. Friend, E. Kaxiras, A density functional study of clean and hydrogen-covered α-MoO 3(010): electronic structure and surface relaxation, J. Chem. Phys. 109 (1998), 6854–6680.
[27] P. Politzer, D.G. Truhlar (Eds.), Chemical Application of Atomic and MolecularElectrostaticPotentials, Plenum, New York, 1981.
[28] E. Scrocco, J. Tomasi, Electronic molecular structure, reactivity and intermolecular forces: aneuristic interpretation by means of electrostatic molecular potentials, Adv. Quantum Chem. 11 (1978) 115–121.
[29] N. Puviarasan, V. Arjunan, S. Mohan, FT-IR and FT-Raman studies on 3-

aminophthalhydrazide and N-aminophthalimide, Turk. J. Chem. 26 (2002) 323.
[30] G. Varsanyi, Vibrational Spectra of Benzene Derivatives, Academic Press, New York, 1969.
[31] V. Krishnakumar, V. Balachandran, T. Chithambarathanu, Density functional theory study of the FT-IR spectra of phthalimide and N-bromophthalimide, Spectrochim. Acta 62A (2005) 918.
[32] V. Krishnakumar, R. John Xavier, Normal coordinate analysis of 2-mercapto and 4, 6-dihydroxy-2-mercapto pyrimidines, Indian J. Pure Appl. Phys. 41 (2003) 597.
[33] V. Krishnakumar, V.N. Prabavathi, Simulation of IR and Raman spectral based on scaled DFT force fields: a case study of 2-amino 4-hydroxy 6-trifluoromethylpyrimidine, with emphasis on band assignment, Spectrochim. Acta 71 (2008) 449. Part A.
[34] F. Weinhold, C.R. Landıs, Natural Bond Orbitals and Extensions of Localized Bonding Concepts, Chem. Edu. Res. Prac. Eur. 2 (2) (2001) 91–104.
[35] V. Arjunan, A. Raj, C.V. Mythili, S. Mohan, Vibrational, electronic and quantum chemical studies of 5-benzimidazole carboxylic acid, J. Mol. Struct. 1036 (2013) 326–340.
[36] T.S. Xavier, N. Rashid, I.H. Joe, Vibrational spectra and DFT study of anticancer active molecule 2-(4-Bromophenyl)-1H-benzimidazole by normal coordinate analysis, Spectrochim. A 78 (2011) 319–326.
[37] N.T.A. Ghani, A.M. Mansour, Molecular structures of 2-arylaminomethyl-1H-benzimidazole: spectral, electrochemical, DFT and biological studies, SpectrochimicaActaPart A 91 (2012) 272–284.
[38] N.T.A. Ghani, A.M. Mansour, Molecular structure of 2-chloromethyl-1H-benzimidazole hydrochloride: single crystal, spectral, biological studies, and DFT calculations, Spectrochim. A 86 (2012) 605–613.
[39] Z. Cinar, M. Karabacak, M. Cinar, M. Kurt, P. Chinnababu, N. Sundaraganesan, The infrared, Raman, NMR and UV spectra, ab initio calculations and spectral assignments of 2-amino-4-chloro-6-methoxypyrimidine, Spectrochim. A 116 (2013) 451–459.
[40] L.J. Bellamy, R.L. Williams, The NH stretching frequencies of primary amines, Spectrochim. Acta 9 (1957) 341–345.
[41] L.J. Bellamy, The Infrared Spectra of Complex Molecules, vol. 2, Chapman and Hall, London, 1980.
[42] D.N. Sathyanarayana, Vibrational Spectroscopy – Theory and Applications, second ed., New Age International (P) Limited Publishers, New Delhi, 2004.
[43] V. Arjunan, A. Raj, P. Ravindran, S. Mohan, Structure–activity relations of 2-(methylthio) benzimidazole by FTIR, FT-Raman, NMR, DFT and conceptual DFT methods, Spectrochim. Acta A 118 (2014) 951–9654.
[44] N. Sundaraganesan, S. Ilakiamani, P. Subramani, B.D. Joshua, Comparison of experimental and ab initio HF and DFT vibrational spectra of benzimidazole Spectrochim, Spectrochim. Acta A 67 (2007) 628–635.
[45] H.O. Kalinowski, S. Berger, S. Braun, Carbon–13 NMR Spectroscopy, John Wiley and Sons, Chichester, 1988.
[46] K. Pihlaja, E. Kleinpeter (Eds.), Carbon–13 Chemical Shifts in Structural and Sterochemical Analysis, VCH Publishers, DeerfieldBeach, 1994.
[47] I. Fleming, FrontierOrbitals and Organic Chemical Reactions, Wiley, London, 1976.
[48] K. Fukui, Role of frontier orbitals in chemical reactions, Science 218 (1982) 747–754.
[49] J.S. Murray, K. Sen, MolecularElectrostaticPotentials, Concepts and Applications, Elsevier, Amsterdam, 1996.
[50] I. Fleming, FrontierOrbitals and Organic Chemical Reactions, John Wiley and Sons, New York, 1976, pp. 5–27.
[51] J.M. Seminario, RecentDevelopments and Applications of Modern Density-FunctionalTheory, vol. 4, Elsevier, 1996, pp. 800–806.
[52] T. Yesilkaynak, G. Binzet, F. Mehmet Emen, U. Florke, N. Kulcu, H. Arslan, Theoretical and experimental studies on N-(6-methylpyridin-2-yl-carbamothioyl) biphenyl-4-carboxamide, Eur. J. Chem. 1 (2010) 1–5.
[53] E. Scrocco, J. Tomasi, Electronic molecular structure, reactivity and intermolecular forces: aneuristic interpretation by means of electrostatic molecular potentials, Adv. Quantum Chem. 11 (1978) 115–121.
[54] C. Muñoz-Caro, A. Niño, M.L. Sement, J.M. Leal, S. Ibeas, Modeling of protonation processes in acetohydroxamic acid, J. Org. Chem. 65 (2000) 405–410.
[55] P. Politzer, K.C. Daiker, The Force Concept in Chemistry, Van NostrandReinholdCo, 1981.
[56] P. Politzer, P.R. Laurence, K. Jayasuriya, in: J. McKinney (Ed.), Structure Activity Correlation in MechanismStudies and PredictiveToxicology, Special Issue of Environ, 61, 1985, p. 191. HealthPerspect.
[57] P. Politzer, J.S. Murray, in: D.L. Protein, R. Beveridge, R. Lavery (Eds.), Theoretical Biochemistry and MolecularBiophysics: a ComprehensiveSurvey, vol. 2, AdeninePress, Schenectady, NY, 1991, pp. 165–191.
[58] E. Scrocco, J. Tomasi, Topics in CurrentChemistry, vol. 42, SpringerVerlag, Berlin, 1973.
[59] P. Politzer, D.G. Truhlar (Eds.), Chemical Applications of Atomic and MolecularElectrostaticPotentials, PlenumPress, NY, 1981.